Letters

Optimal Design of Diode-Bridge Bidirectional Solid-State Switch Using Standard Recovery Diodes for 500-kV High-Voltage DC Breaker

Xiangyu Zhang, Zhanqing Yu, Zhengyu Chen, Biao Zhao, *Member, IEEE*, and Rong Zeng, *Senior Member, IEEE*

***Abstract*—At present, it is usually necessary to use fast recovery type diodes to cooperate with the fast switching actions of fully controlled devices such as insulated-gate bipolar transistors (IGBTs). However, the specific nature of the working conditions of the diode-bridge bidirectional solid-state switch (DBSS) provides an opportunity to apply standard recovery diodes for this purpose, which helps to reduce the cost of the bidirectional switch. This letter presents the self-oscillation phenomenon that is caused by the recovery processes of the diodes in a DBSS. Then, the recovery effects of these diodes in different topologies are analyzed from the perspective of the DBSS and optimized designs for both the snubber circuit and the energy-absorbing circuit are proposed. A 500-kV dc breaker is realized based on the proposed DBBS using the standard recovery diodes, which can work reliably with IGBTs, and the cost of the resulting dc circuit breakers is greatly reduced.**

***Index Terms*—DC circuit breaker, diode bridge, solid-state switch, standard recovery diode.**

I. Introduction

SOLID-STATE switches (SSs) based on power electronics technology are frequently applied in dc circuit breakers. The SS can be used directly as a solid-state circuit breaker or can be combined with mechanical switches to form a hybrid circuit breaker (HCB) [1]–[3]. Unlike the mechanical switches, which are inherently bidirectional, SSs require considerable costs to achieve bidirectional functionality because all conventional high-voltage power devices, such as insulated-gate bipolar transistors (IGBTs) or integrated gate-commutated thyristors (IGCTs) [4], [5], are asymmetrical. The main solution used at present for a bidirectional SS is antiseries connection of reverse conducting devices [6]. The full-H-bridge structure described in [7] is also a variant of the antiseries-type structure. Another solution is to use antiparallel connection of reverse blocking devices [8]. Both these solutions double the number of fully controlled devices, greatly increasing the cost of the bidirectional SS. The diode-bridge bidirectional solid-state switch (DBSS) thus represents a more cost-effective choice. The bidirectional functionality can be realized by simply adding four diodes to a unidirectional SS.

TABLE I
Performance Comparison

Items	Conduction loss	Max. turn-off di/dt	Cost (p.u.)
Standard recovery diode	Low	Around 50 A/us	0.04
Fast recovery diode	High	1000~5000 A/us	0.2
Cost of anti-series type bidirectional SS (two IGBTs)			2
Cost of DBSS using fast recover diodes			1.8
Cost of DBSS using standard recover diodes			1.16

The commonly used power diodes can be divided into two categories: standard recovery diodes (or rectifier diodes) and fast recovery diodes. Standard recovery diodes are mainly used in low-frequency applications, such as utility frequency power rectifiers. Fast recovery diodes can attain the reverse blocking state much more quickly so they can work reliably in fast switching applications, as complementary diodes for the high-speed devices (IGBTs or IGCTs) used in converters [9], [10].

From engineering experience, the diodes that are used in DBSSs are preferably the fast recovery type because the rapid switch actions (>2000 A/μs) of IGBTs can cause quite severe transient stresses on the diodes. However, in DBSS applications, the cost of four added fast recovery diodes is close to that of one IGBT. Therefore, the total cost is not significantly reduced when compared with that of the original antiseries-type SS.

In contrast, as shown in Table I, the cost of standard recovery diodes is much lower, which can effectively reduce the total cost of the DBSS. In addition, the conduction losses of standard recovery diodes are also lower, making them more suitable for high-current switch applications. With regard to the recovery problem, it should be noted that the diodes in a DBSS do not need to undergo long-term repeated commutations with the IGBTs like those in the converter because the breakers in power system are inactive for most of the time. And there is no research or evidence to date to indicate that the DBSS working condition requires diodes to have fast recovery characteristics.

Manuscript received May 10, 2019; revised June 14, 2019 and July 11, 2019; accepted July 21, 2019. Date of publication July 23, 2019; date of current version November 12, 2019. This work was supported in part by National Key Research and Development Program of China under Grant 2018YFB0904603 and in part by the National Natural Science Foundation of China under Grant 51837006. *(Corresponding authors: Rong Zeng; Zhanqing Yu.)*

The authors are with the Department of Electrical Engineering, Tsinghua University, Beijing 100084, China (e-mail: zhangxiangyu11@gmail.com; yzq@tsinghua.edu.cn; chenzhen14@mails.tsinghua.edu.cn; zhaobiao112904829@126.com; zengrong@tsinghua.edu.cn).

Color versions of one or more of the figures in this paper are available online at http://ieeexplore.ieee.org.

Digital Object Identifier 10.1109/TPEL.2019.2930739

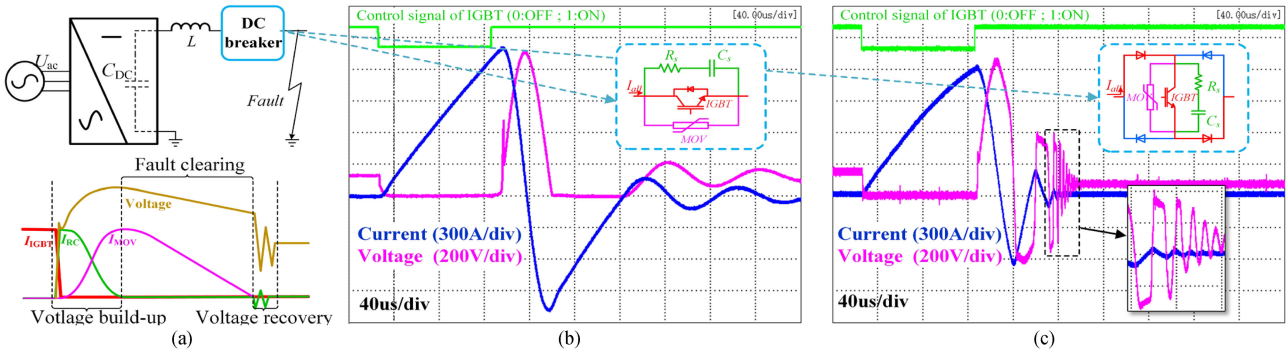

Fig. 1. Self-oscillation phenomenon in DBSS. (a) Working process of the SS. (b) Experimental result of the unidirectional SS. (c) Experimental result of the DBSS using standard recovery diodes.

In this letter, the recovery effect is analyzed from the perspective of the DBSS and some interesting phenomena are discovered. In fact, the use of standard recovery diodes in the DBSS will certainly cause device damage in some cases, but this problem can be effectively solved using the measures proposed in this letter. The results of this research can greatly reduce the cost of a bidirectional SS while maintaining its reliability, and the designed DBSS has been applied in a 500-kV dc HCB, which comprises a mechanical switch branch, a SS branch, and a current-commutation equipment. Application of standard recovery diodes can save approximately 30% of the semiconductor costs.

II. Self-Oscillation Phenomenon Caused by Recovery Process of Diodes in DBSS

An SS generally contains three parts: the fully-controlled power devices (usually IGBTs), the snubber circuits [resistor–capacitor (*RC*) circuits] the energy-absorbing circuits [metal oxide varistors (MOVs)]. As shown in Fig. 1(a), the voltage source converter-based dc system can be equivalent to a large capacitor (the converter) in series with an inductor (the flat wave reactor and the transmission line). When the SS of the dc circuit breaker needs to cut the current OFF, the IGBT first turns OFF. The current then flows to the snubber circuit and charges the snubber capacitor C_s (voltage build-up process). When the voltage rises above the system voltage, the current begins to drop (fault clearing process). The MOV eventually limits the overvoltage and absorbs the energy. When the current drops to zero, the C_s is still charged with the overvoltage. Therefore, the C_s may undergo charging and discharging processes with the system until the voltage is balanced (voltage recovery process).

Fig. 1(b) shows the turn-OFF waveform of a unidirectional SS. The figure shows that the residual voltage of C_s generates a significant resistor–inductor–capacitor (*RLC*) oscillation during the voltage drop process. When four standard recovery diodes are added to the original SS to form the DBSS, an interesting phenomenon occurs. As shown in Fig. 1(c), the switch experiences an unexpectedly violent oscillation process after the IGBT is turned OFF. This mechanism differs from the previous *RLC* oscillation. The recovery process of the diodes makes the voltage recovery process complex. In practice, this phenomenon will not only cause the diodes to withstand excessive reverse currents, but it will also generate electromagnetic interference in the control units.

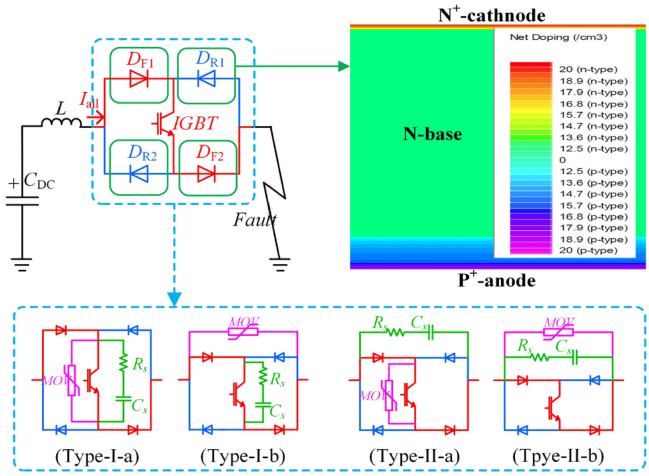

Fig. 2. Transient analysis models of different DBSS topologies.

III. Comprehensive Transient Analysis of Diode Recovery Effects in Different Topologies

A. Different DBSS Topologies

The abnormal oscillation of the DBSS observed in the previous section occurs because the *RC* circuit, which should oscillate directly with the system, is limited by the diode bridge. In fact, regardless of whether the snubber circuit (or the energy-absorbing circuit) is placed inside or outside the diode bridge, its effect on the IGBT will not change. Therefore, depending on the location of the *RC* circuit, the DBSS can have two types of topologies (Type-I and Type-II), and each topology type can be further divided into two subtypes depending on the location of the MOV. As shown in Fig. 2, the transient processes of the different DBSS topologies were simulated using Silvaco TCAD software with a finite element model of the diodes. To make the recovery process more obvious, the minority carrier lifetime of the diodes is set

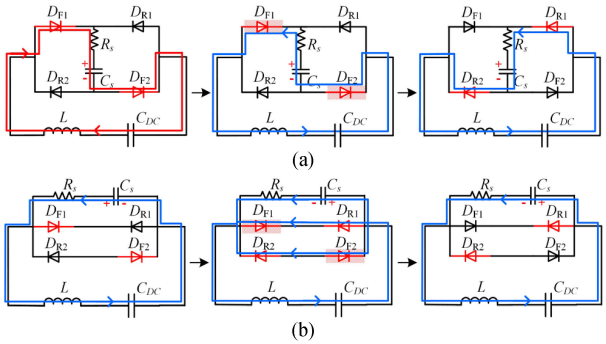

Fig. 3. Diodes recovery in different topologies. (a) Type-I. (b) Type-II.

at 400 μs. For the circuit part, the $C_{\rm DC}$ is set as 400 μF and is precharged of 1000 V. The L is 100 μF. And the *RC* snubber is chosen as 0.5 Ω and 5 μF, respectively. The reference voltage of MOV is 2.4 kV, and the residual voltage of MOV is 4 kV at 10 kA.

B. Diode Recovery Effect in Type-I DBSS

The transient recovery processes of the Type-I DBSS have been illustrated in Fig. 3(a). Before the voltage recovery process, the forward diodes ($D_{\rm F1}$ and $D_{\rm F2}$) are conducting the current and accumulate large numbers of carriers, whereas the reverse diodes (D_{R1} and $\rm D_{R2}$) only withstand the voltage. Therefore, the forward diodes are in a recovery state and cannot establish a reverse voltage. Then, as shown in Fig. 3(a), C_s can discharge to the external system through the forward diodes. When the diodes then complete the reverse recovery process and block the current, the energy has already been stored on the external inductor; the current thus begins to flow through the reverse diodes, which causes C_s to be charged again. The module voltage thus flips instantaneously. After that, as the reverse diodes have just passed the current, a symmetrical process will occur again but at lower energy. The two processes will continue to repeat until the unbalanced voltage is blocked at some point.

Fig. 4(a) shows the simulation results for the Type-I-a topology. The total current ($I_{\rm all}$) and total voltage are basically consistent with the experimental waveform shown in Fig. 1(d). Each recovery process is weaker than the last, and the oscillation frequency becomes higher and higher. Besides, the current of forward diodes (I_{FD}), the current of reverse diodes (I_{RD}), and the current of *RC* snubber ($I_{\rm RC}$) are also given in the simulations.

In the Type-I-b topology [see Fig. 4(b)], the MOV is moved from the inside to the outside of the diode bridge. The difference here is that no current flows through the forward diodes during the fault clearing process, resulting in longer recombination times for the carriers in the forward diodes. The diodes' reverse current in Type-I-b is obviously less than that in Type-I-a. As a result, the residual voltage on C_s is higher and the voltage flip frequency also increases.

C. Diode Recovery Effect in Type-II DBSS

Unlike the Type-I case, the *RC* circuit is moved to the outside of the diode bridge in the Type-II topology. Therefore, the recovery process is completely different. As shown in Fig. 3(b), at the beginning of the voltage drop process, the *RC* circuit can discharge directly to the system, which represents an *RLC* oscillation. When the voltage across the capacitor oscillates in the reverse direction, because the forward diodes have just carried the fault current in the previous process, D_{F1} and D_{F2} then form temporary paths with D_{R1} and D_{R2}, respectively. The current that flows through these two paths is not only the reverse current of the forward diodes but is also the forward current of the reverse diodes. Therefore, after half an oscillation period, the same process occurs symmetrically.

The simulation results for the Type-II-a [see Fig. 5(a)] and Type-II-a [see Fig. 5(b)] topologies both verify the above analysis. During the voltage drop process, the waveform is roughly that of an *RLC* oscillation, except that the voltage waveform is discontinuous every time it crosses zero. The currents also appear simultaneously on the diodes. The recovery process of Type-II-a is more obviously due to the inside placed MOV.

IV. Optimal DBSS Design

A. DBSS Topology Selection

The previous analysis showed that placing the MOV inside the diode bridge not only causes the forward diodes to withstand increased currents during the fault clearing process but also exacerbates the subsequent reverse recovery process. Therefore, Type-I-a and Type-II-a topologies are excluded first. In addition, because the internal *RC* circuit will cause high-frequency self-oscillation, Type-I topologies are also not recommended. Type-II-b is thus the best DBSS topology.

However, from a dc system perspective, Type-II is worse than Type-I in terms of the time needed to clear the fault completely (as shown by the current waveforms in Figs. 4 and 5) because the external *RC* circuit will cause the current to continue to oscillate. In particular, when the system inductance is high, the damping coefficient of the oscillation will become very small. The oscillation may last for hundreds of milliseconds, thus affecting the system reclosing time.

B. Fast Decay Design Based on MOV-C Snubber

Increasing the resistance has an effect on the current decay rate, but it will also cause higher voltage spikes and may thus damage the device. To solve this problem, a novel fast decay snubber is designed to cooperate with the SS. R_s in the *RC* circuit is replaced with another varistor $R_{\rm mov}$, and the $R_{\rm mov}$'s parameters are specifically designed to make the equivalent resistance at the maximum current (i.e., the current that the SS needs for cutoff) the same as the original R_s. Therefore, the snubber circuit not only maintains its original performance during the cutoff process but also shows a much higher damping coefficient in subsequent oscillations because of the nonlinear characteristics of the MOV. In addition, this fast decay design also reduced the zero crossings in the oscillation and further suppressed the recovery processes in Type-II-b. It should be noted that after using MOV-C snubber, the transient turn-OFF power of the IGBT will increase slightly, so the gate-driver's

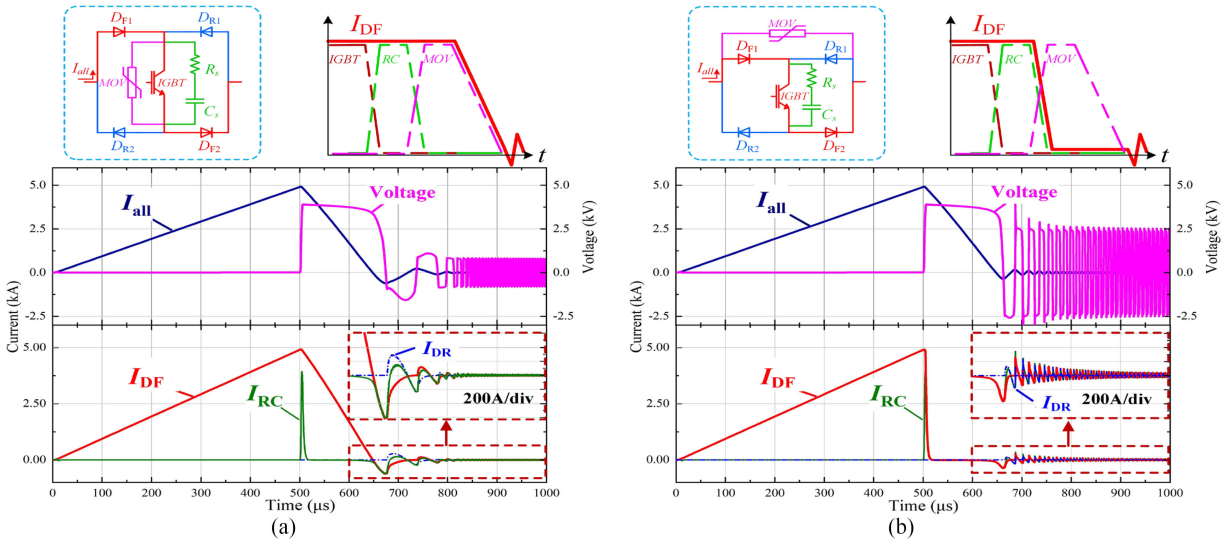

Fig. 4. Simulation results of *RC*-inside Type-I topologies. (a) Type-I-a with internal MOV. (b) Type-I-b with external MOV.

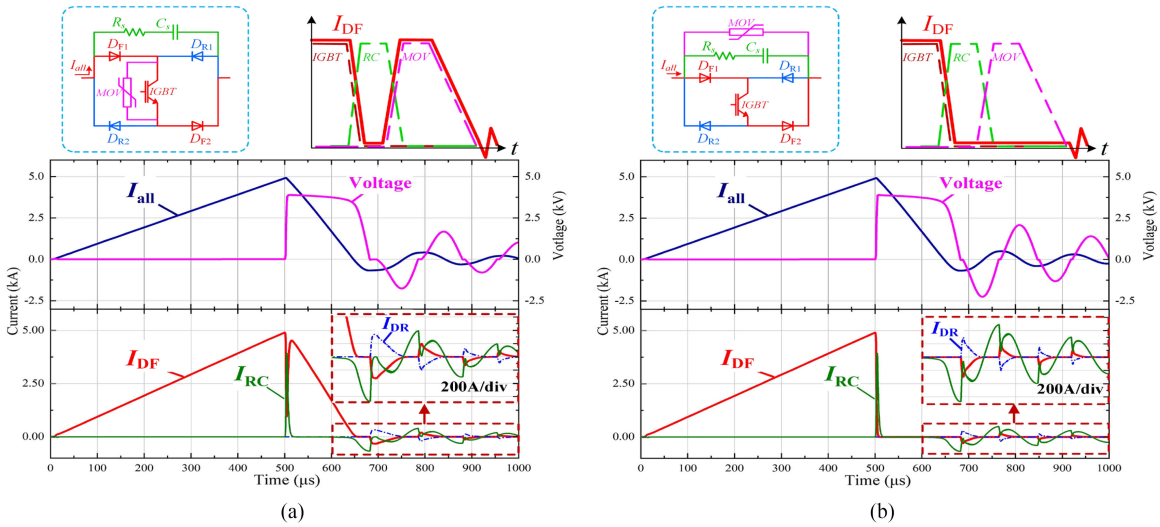

Fig. 5. Simulation results of *RC*-outside Type-II topologies. (a) Type-II-a with internal MOV. (b) Type-II-b with external MOV.

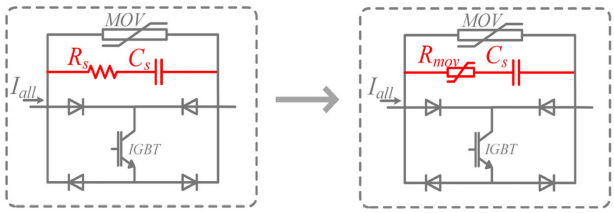

Fig. 6. Fast decay design based on the MOV-C snubber.

resistance should be appropriately reduced as a compensation measure.

C. Parameters Design of MOV-C Snubber

For the *RC* snubber and MOV based SS, a detailed parameters design method has been proposed in [11]. The parameters of

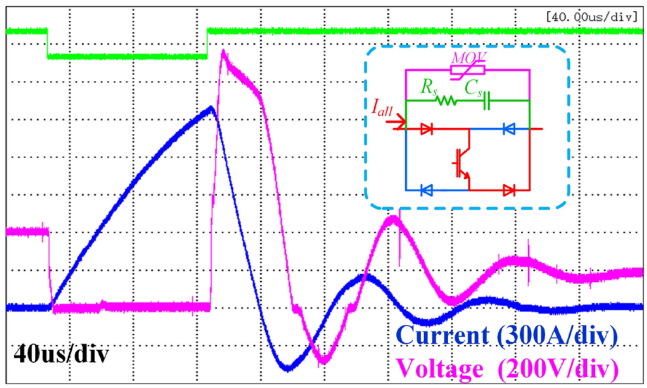

Fig. 7. Experimental results for DBSS using Type-II-b topology.

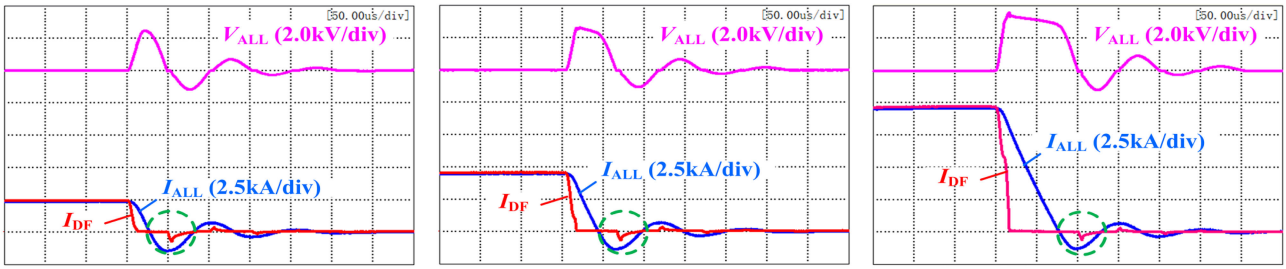

Fig. 8. Reverse process of Type-II-b topology for different current levels. (a) 2.5 kA. (b) 5 kA. (c) 10 kA.

snubber are related to the specifications of IGBT and its protection MOV. Based on the derivation in [11], R_s and C_s were deliberately decoupled. Thus, in MOV-C snubber, C_s does not need to be changed

$$C_s \geq \frac{I_c \cdot t_{\text{res}} \cdot \alpha_{\max}(K)}{U_{\text{res}(I_c, t_{res})}} \tag{1}$$

where I_c denotes the rated maximum turn-OFF current, t_{res} denotes the nominal front wave time of the MOV, and the U_{res} denotes the residual voltage of the MOV under a current of I_c with a front time of t_{res}. $\alpha_{\max}$ is a correction factor related to the nonlinearity of the MOV, and K is the residual voltage ratio

$$\alpha_{\max}(k) = \frac{0.24}{k - 1.3} + 0.83 \ \ (k \geq 1.4). \tag{2}$$

For the resistance of the snubber, R_s needs to be large enough to limit the surge current in the turn-ON process. And it also cannot be too large, otherwise it would affect the snubber function of the C_s when IGBT is switching OFF. The upper and lower boundaries of R_s are given as

$$\frac{U_{\text{ref}}}{I_{\text{surge}}} \leq R_s \leq \frac{U_{\text{ref}}}{I_c} \tag{3}$$

where I_{surge} denotes the maximum surge current of the IGBT and U_{res} denotes the reference voltage of the MOV, which is also the SS module's dc rated voltage of V_{dc}.

Therefore, in MOV-C snubber, we can make the equivalent resistance of R_{mov} under the voltage of V_{dc} equal to the R_s, thus achieving the same effect as before

$$R_{\text{mov}}(@V_{\text{dc}}) = R_s.a. \tag{4}$$

V. Experimental

The cutoff experiment performed in Section II [see Fig. 1(c)] is performed again using the recommended Type-II-b topology. As shown in Fig. 7, the results are basically the same as those of the simulation. There are no high-frequency oscillations any more. Note that the voltage waveform is discontinuous when it crosses zero; this is caused by the standard recovery diodes. Because the reverse recovery process is not very intense and does not occur repeatedly, the diodes remain safe. Fig. 8 shows the recovery process of Type-II-b for different current levels. If the system parameters are the same, the larger the current, the longer the energy consumption of the arrester, resulting in longer recombination times for the carriers in the diodes. Therefore, the diode recovery process (the area of the reverse part of I_{FD}) will slightly weaken as the current increases.

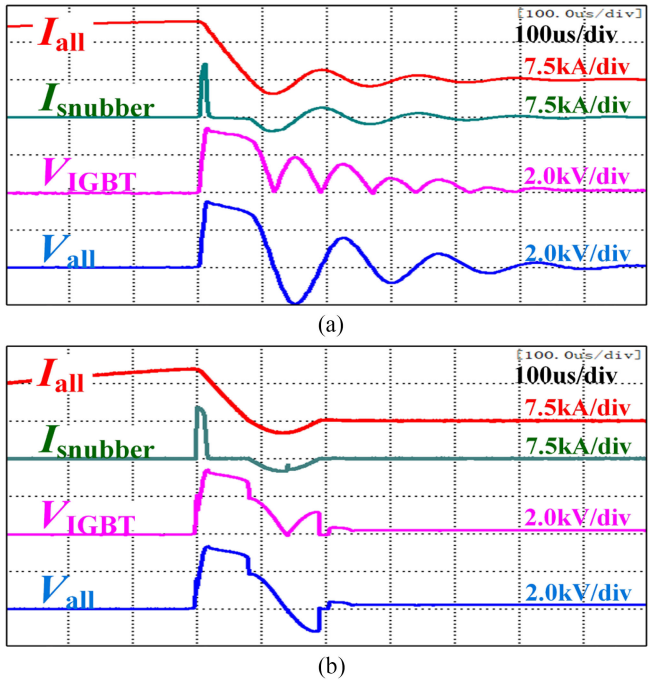

Fig. 9. Experiment of fast decay design. (a) *RC* snubber. (b) MOV-C snubber.

The fast decay design is then also verified experimentally. When using the *RC* snubber [see Fig. 9(a)], the system will still have an oscillating current after the MOV has absorbed the energy. In addition, after using the MOV-C snubber [see Fig. 9(b)], the IGBT is still able to turn OFF the current reliably, and the previous current oscillations are significantly suppressed.

Based on the bidirectional design principles presented in this letter, the SS part of a 500 kV/25 kA hybrid dc breaker has been developed [11]. As shown in Fig. 10, this breaker consists of 320 DBSS modules and 1280 diodes. The circuit breaker has just completed type tests, and the experimental waveform of the solid-state part is shown in Fig. 11.

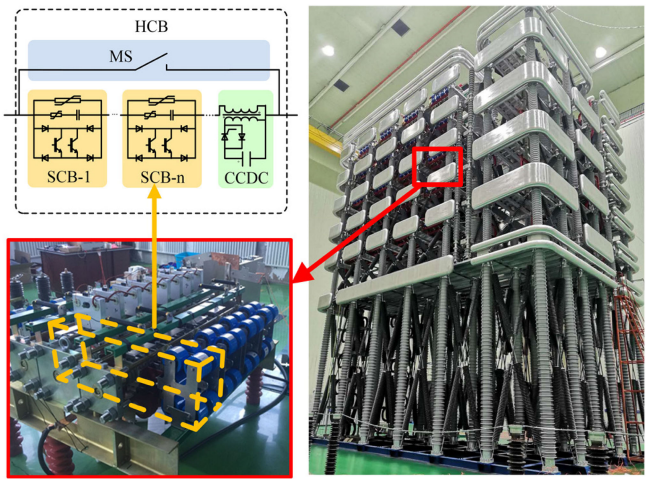

Fig. 10. Application of DBSS using standard recovery diodes in 500-kV hybrid dc circuit breaker.

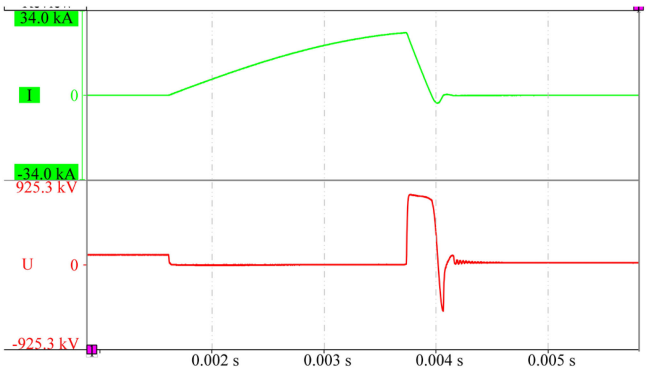

Fig. 11. Experimental waveforms of 500-kV bidirectional SS.

VI. Conclusion

This letter studies the application of a diode-bridge bidirectional structure in SSs and the structure's diode recovery characteristics. In summary, the location of the *RC* circuit affects the diode recovery mechanism, and the MOV location affects the severity of the diode recovery. The diode recovery process is greatly suppressed if the *RC* circuit and the MOV are both placed outside the bridge. Therefore, standard recovery diodes with low costs and higher currents can be used instead of fast recovery diodes in SSs. In addition, a new MOV-C snubber is also proposed to solve the current decay issue. A 500-kV dc breaker is realized based on the DBBS using the standard recovery diodes, which can work reliably with IGBTs, and the cost of the dc circuit breaker is greatly reduced.

References

[1] N. Flourentzou, V. G. Agelidis, and G. D. Demetriades, "VSC-based HVDC power transmission systems: An overview," *IEEE Trans. Power Electron.*, vol. 24, no. 3, pp. 592–602, Mar. 2009.

[2] A. Abramovitz and K. M. Smedley, "Survey of solid-state fault current limiters," *IEEE Power Electron.*, vol. 27, no. 6, pp. 2770–2782, Jun. 2012.

[3] Z. A. Shukla and G. D. Demetriades, "A survey on hybrid circuit-breaker topologies," *IEEE Trans. Power Del.*, vol. 30, no. 2, pp. 627–641, Jul. 2014.

[4] Z. Chen *et al.*, "Analysis and experiments for IGBT, IEGT, and IGCT in hybrid DC circuit breaker," *IEEE Trans. Ind. Electron.*, vol. 65, no. 4, pp. 2883–2892, Apr. 2018.

[5] B. Zhao *et al.*, "A more prospective look at IGCT: Uncovering a promising choice for dc grids," *IEEE Ind. Electron. Mag.*, vol. 12, no. 3, pp. 6–18, 2018.

[6] J. Hafner, "Proactive hybrid HVdc breakers—A key innovation for reliable hvdc grids," in *Proc. CIGRE Bologna Symp.*, 2011, pp. 1–8.

[7] W. Zhou *et al.*, "Development and test of a 200 kV full-bridge based hybrid HVDC breaker," in *Proc. 17th Eur. Conf. Power Electron. Appl.*, 2015, pp. 1–7.

[8] C. Meyer *et al.*, "Solid-state circuit breakers and current limiters for medium-voltage systems having distributed power systems," *IEEE Power Electron.*, vol. 19, no. 5, pp. 1333–1340, Sep. 2004.

[9] B. Zhao *et al.*, "Practical analytical model and comprehensive comparison of power loss performance for various MMCs based on IGCT in HVDC application," *J. Emerg. Sel. Topics Power Electron.*, vol. 7, no. 2, pp. 1071–1083, Feb. 2019.

[10] R. Zeng *et al.*, "Integrated gate commutated thyristor-based modular multilevel converters: A promising solution for ultra-high-voltage dc applications," *IEEE Ind. Electron. Mag.*, vol. 13, no. 2, pp. 4–16, 2019.

[11] X. Zhang *et al.*, "Modular design methodology of DC breaker based on discrete metal oxide varistors with series power electronic devices for HVDC application," *IEEE Trans. Ind. Electron.*, vol. 66, no. 10, pp. 7653–7662, Oct. 2019.